Published in final edited form as:
*Stem Cells*. 2009 April ; 27(4): 866–877. doi:10.1002/stem.2.

# Stem Cell Property of Postmigratory Cranial Neural Crest Cells and Their Utility in Alveolar Bone Regeneration and Tooth Development

**Il-Hyuk Chung**[a,b], **Takayoshi Yamaza**[a], **Hu Zhao**[a], **Pill-Hoon Choung**[b], **Songtao Shi**[a], and **Yang Chai**[a]

[a]Center for Craniofacial Molecular Biology, School of Dentistry, University of Southern California, Los Angeles, California, USA

[b]Department of Oral and Maxillofacial Surgery, Seoul National University Boramae Hospital, Seoul, Republic of Korea

## Abstract

The vertebrate neural crest is a multipotent cell population that gives rise to a variety of different cell types. We have discovered that postmigratory cranial neural crest cells (CNCCs) maintain mesenchymal stem cell characteristics and show potential utility for the regeneration of craniofacial structures. We are able to induce the osteogenic differentiation of postmigratory CNCCs, and this differentiation is regulated by bone morphogenetic protein (BMP) and transforming growth factor-*β* signaling pathways. After transplantation into a host animal, postmigratory CNCCs form bone matrix. CNCC-formed bones are distinct from bones regenerated by bone marrow mesenchymal stem cells. In addition, CNCCs support tooth germ survival via BMP signaling in our CNCC-tooth germ cotransplantation system. Thus, we conclude that postmigratory CNCCs preserve stem cell features, contribute to craniofacial bone formation, and play a fundamental role in supporting tooth organ development. These findings reveal a novel function for postmigratory CNCCs in organ development, and demonstrate the utility of these CNCCs in regenerating craniofacial structures.

### Keywords

Cranial neural crest cells; Tooth; Bone morphogenetic protein; Alveolar bone; Smad4

## Introduction

The vertebrate neural crest is a multipotent cell population derived from the lateral ridges of the neural plate. This multipotency is modified by growth factor signaling pathways and their



Correspondence: Yang Chai, DDS, Ph.D., Center for Craniofacial Molecular Biology, School of Dentistry, University of Southern California, 2250 Alcazar Street, CSA 103, Los Angeles, California 90033, USA. Telephone: +323-442-3480; Fax: +323-442-2981; ychai@usc.edu.

Author contributions: I.-H.C.: conception and design, provision of study material, collection and assembly of data, data analysis and interpretation, manuscript writing; T.Y.: provision of study material, collection and assembly of data, data analysis and interpretation; H.Z.: provision of study material, collection and assembly of data, data analysis and interpretation; P.-H.C.: administrative support; S.S.: conception and design, collection and assembly of data, data analysis and interpretation, manuscript writing; Y.C.: conception and design, financial support, administrative support, data analysis and interpretation, manuscript writing, final approval of manuscript.

Disclosure of Potential Conflicts of Interests

The authors indicate no potential conflicts of interest.

See www.StemCells.com for supporting information available online.

downstream transcription factors, such that neural crest cells (NCCs) eventually become committed to one of a number of different cell types [1-3]. Derivatives of NCCs include sensory neurons, autonomic neurons, glia, melanocytes, adrenal medulla cells, and smooth muscle cells. During craniofacial development, cranial neural crest cells (CNCCs) migrate ventrolaterally as they populate the branchial arches. CNCC migration from the midbrain and anterior hindbrain into the first branchial arch begins around the 4-somite stage. Eventually, those CNCCs give rise to mesenchymal structures such as cartilage, bone, and teeth, in addition to neural tissues [4-7].

Previous studies, in which individual premigratory or migratory NCCs are labeled with dye and the fates of their descendants are then followed, have suggested that NCCs can give rise to multiple types of derivatives from a single progenitor cell [8,9]. Clonal analysis confirms this finding and demonstrates that these cells self-renew and share some of the unique characteristics of stem cells [10]. However, some individual NCCs give rise to only one type of derivative. Thus, it has been proposed that even at the onset of migration, the neural crest is composed of a heterogeneous population of cells with different proliferation and differentiation potentials [11]. Interestingly, multipotent NCCs have also been identified in sites where postmigratory NCCs reside [12,13]. This implies that some of the premigratory NCCs maintain their multipotent differentiation ability and undergo self-renewal or become quiescent after migration. Others may restrict their differentiation potential progressively and commit to one specific lineage [6]. The extent to which postmigratory CNCCs maintain stem cell characteristics is unknown.

Among many tissues that originated from CNCCs, tooth, and alveolar bone are structures that are only found in the craniofacial region. These two structures have an interdependent relationship. Alveolar bone provides the support for a functional dentition, and it can be reshaped based on the precise needs of the tooth. Development of the alveolar bone involves CNCC-derived mesenchymal cell condensation to form the dental sac, osteoid deposition and mineralization [4,14]. A well-defined intramembranous bony socket, consisting of differentiating osteoblasts that are enriched in bone matrix, is built surrounding the developing tooth [15]. Clinically, loss of a tooth results in the absorption of alveolar bone, suggesting that there is an intimate relationship between alveolar bone and tooth development. Thus, to design a biological solution to regenerate a tooth, it is critical to generate alveolar bone that is fully integrated with and provides support for the newly formed tooth. The knowledge of the manner in which CNCCs differentiate into osteoblasts and the molecular mechanism that regulates the formation of alveolar bone is critical for the regeneration of functional dentition.

Recently, we described a cell culture system for generating a pure population of CNCCs using the *Wnt1-Cre;R26R* mouse model, optimized to support the proliferation of the first branchial arch CNCCs [16]. In this model, cultured CNCCs can give rise to neurons, glial cells, osteoblasts, and other cell types, faithfully mimicking the differentiation process of postmigratory CNCCs in vivo [16]. On the basis of these findings, we have now investigated specific characteristics of postmigratory first branchial arch CNCCs and evaluated the molecular regulatory mechanism of differentiation through the culture and transplantation of CNCCs from *Wnt1-Cre;R26R* mice. In addition, we have developed a method for co-transplantation of CNCCs and tooth germs subcutaneously, after which we detected continued tooth development in CNCC-supported tooth germ. These findings suggest that cross-talk between postmigratory CNCCs and tooth germ play a key role in the development of alveolar bone and tooth.

## Materials and Methods

### Postmigratory CNCC Culture and Generation of Mutant Mice

We mated *Wnt1-Cre* and *R26R* conditional reporter mice [17,18] to generate transgenic mice with NCCs that could be labeled indelibly with $\beta$-galactosidase [4]. *Wnt1-Cre;R26R* heterozygous embryos were removed at embryonic day 10.5. The first branchial arches were dissected, and postmigratory CNCCs were collected and cultured.

We mated *Tgfbr2*$^{fl/+}$*;R26R;Wnt1-Cre* with *Tgfbr2*$^{fl/fl}$*;R26R* mice to generate *Tgfbr2*$^{fl/fl}$*;R26R;Wnt1-Cre* null alleles [19]. In addition, we mated *Smad4*$^{fl/+}$*;R26R;Wnt1-Cre* with *Smad4*$^{fl/fl}$*;R26R* mice to generate *Smad4*$^{fl/fl}$*;R26R;Wnt1-Cre* null alleles [20]. Normal culture medium consisted of MEM-alpha (Invitrogen, Carlsbad, CA, http://www.invitrogen.com) containing 20% fetal bovine serum (Equitech-Bio Inc., Kerrville, TX, http://www.equitech-bio.com) 2 mM L-glutamine, 55 nM 2-mercaptoethanol and 25U/ml penicillin and 25 $\mu$g/ml streptomycin sulfate (Invitrogen).

### Culture of Mandibular MSCs and BMMSCs

For the culture of mandiblular mesenchymal stem cells (MSCs), mandibles were dissected from 7- to 8-week-old *Wnt1-Cre;R26R* mice, chopped into small pieces and digested with an equal mixture of collagenase (2 mg/ml; Sigma, St. Louis, MO, http://www.sigmaaldrich.com) and dispase (4 mg/ml; Sigma) at 37°C for 1 hour. After counting viable cells, $5 \times 10^5$ cells were plated into 10-cm culture dish. In addition, for the culture of bone marrow mesenchymal stem cells (BMMSCs), tibias and femurs were dissected from 8- to 10-week-old mice. The bone marrow was flushed out and centrifuged. After counting viable cells, $1 \times 10^6$ cells were plated per 10-cm culture dish. Normal culture medium was also used for mandibular MSC and BMMSC culture.

### Analysis of Colony Formation and Cell Proliferation

To assess colony formation, $5 \times 10^3$ of CNCCs were seeded into 10-cm culture dishes and cultured. To confirm CNCC identity, single colonies were examined to detect CNCC-specific $\beta$-galactosidase activity. Cell proliferation activity was monitored by administration of 5-bromo-2′-deoxyurine (BrdU; Zymed, San Francisco, CA, http://www.bioresearchonline.com). After 20 hours, BrdU-labeled cells were detected using a BrdU Labeling and Detection kit (Zymed).

### Immunocytochemistry of Cultured Postmigratory CNCCs

To characterize the colonies originating from postmigratory CNCCs, neurofilament (NF) 145 (rabbit anti-mouse, 1:400; Chemicon, Temecula, CA, http://www.chemicon.com), $\alpha$-smooth muscle actin ($\alpha$-SMA, goat anti-mouse, 1:400; Sigma), S100 (rabbit anti-mouse, 1:400; Sigma), Type I collagen (rabbit anti-mouse, 1:500; Sigma), nerve trophic receptor (NTR) p75 (rabbit anti-mouse, 1:400; Chemicon), and Nestin (anti-mouse, 1:400; Chemicon) were assayed using immunocytochemistry.

### Fluorescence-Activated Cell Sorting and Immunophenotyping

Growing cells were stained with fluorescein di-$\beta$-D-galactopyranoside (FDG) for the detection of $\beta$-galactosidase and fluorescence-activated cell sorting (FACS) was performed. For the evaluation of MSC markers, the cultured cells were incubated with FDG and phycoerythrin (PE)-conjugated anti-mouse CD44, Sca-1 (stem cell antigen-1), CD29, CD90.2, CD49e, CD13, CD18, CD34, c-Kit (CD 117), CD45, SSEA4 (stage-specific embryonic antigen 4), OCT4 (Octan 4), or isotype control of IgG (BD Pharmingen, San Diego, CA,

http://www.bdbiosciences.com/index[lowen]us.shtml), and flow cytometry analysis was performed according to standard procedures.

### Multipotent Differentiation

Differentiation potential of the CNCCs to undergo osteogenesis, adipogenesis, and chondrogenesis was examined, as previously described [21,22] (supporting information).

### In Vivo Transplantation of Cultured Cells

Cultured cells ($2.0 \times 10^6$) were mixed with 40 mg hydroxyapatite/tricalcium phosphate (HA/TCP) ceramic powder (Zimmer, Warsaw, IN, http://www.zimmer.com), and the pellet of HA/TCP with adherent cells was then transplanted subcutaneously into the dorsal surface of 8-week-old female immunocompromised beige mice (NIH-bg-nu/v-xid; Harlan Sprague Dawley, Indianapolis, MN, http://www.harlan.com). In some cases, pellets were mixed with bone morphogenetic protein 2 (BMP2; 10 $\mu$g/ml), transforming growth factor-$\beta$2 (TGF-$\beta$2; 10 $\mu$g/ml), or fibroblast growth factor 9 (FGF9; 10 $\mu$g/ml, R&D Systems, http://www.rndsystems.com) beads, and then transplanted [19]. In some experiments, cultured cells were loaded onto $10 \times 10$-mm$^2$ collagen-based gelatin sponge (Gelfoam, Pharmacia & Upjohn, Somerset, NJ, http://www.nndb.com) or mixed with 1 ml of basement membrane matrix, (Matrigel, BD biosciences), and then transplanted. In addition, to evaluate the regeneration of a craniofacial bone defect, we made defects larger than the critical size defect (diameter 3 mm) in mouse calvaria and transplanted cultured cells ($4.0 \times 10^6$ cells) mixed with 40 mg HA/TCP into the host. The samples were harvested at 8 weeks post-transplantation.

### Transplantation of Tooth Germs and Cultured Cells

Mandibular molar tooth germs were dissected from wild-type mouse embryos at E13.5, then transplanted subcutaneously with $4.0 \times 10^6$ cells and HA/TCP into the dorsal surface of immunocompromised mice. In some cases, pellets containing tooth germs were mixed with BMP4- (100 $\mu$g/ml), Noggin- (100 $\mu$g/ml), Activin$\beta$A- (10 $\mu$g/ml), FGF2- (0.5 $\mu$g/ml), or FGF4- (200 $\mu$g/ml; R&D Systems) beads before transplantation. The samples were harvested at 8 weeks post-transplantation.

### Detection of $\beta$-Galactosidase (*LacZ*) Activity

Cultured cells and harvested transplants were fixed with 0.2% glutaraldehyde. Tissue transplant decalcification was performed with 5% EDTA and embedded in OCT medium (Sakura Finetek, Torrance, CA, http://www.sakura.com). Sections and cultured cells were stained with X-gal ($C_{14}H_{15}BrClNO_6$, USB Co, Cleveland, OH, http://www.usb.com) according to standard procedure as previously described [4,16].

### Statistical Analysis

Student's *t* test was applied for statistical analysis. A *p* value of less than .05 was considered statistically significant.

## Results

### Stem Cell Characteristics of Postmigratory CNCCs

To characterize postmigratory CNCCs, we generated a single cell suspension from the first branchial arch of *Wnt1-Cre;R26R* embryos at E10.5. When cultured at a low cell density, a small population (0.19% ± 0.07%) of postmigratory CNCCs formed adherent cell colonies (Fig. 1A). These colonies were heterogeneous in size and cell density (supporting information Fig. 1A). These colony-forming cells were positive for CNCC specific $\beta$-galactosidase activity after X-gal staining, and NTR p75 (89.6% ± 3.3%), another NCC marker, based on

immunostaining (supporting information Fig. 1B). We detected $\alpha$-SMA (60% ± 5%) and type 1 collagen (30% ± 6%) expressing colonies, which show MSC characteristics. By changing to neural differentiation culture media, as previously described [16], we also detected NF145, and S100 expressing colonies (Fig. 1B). After 3 days culture with normal culture medium, we detected CNCCs from multiple colonies that expressed Nestin (73.9% ± 2.0%), a neural stem cell marker (supporting information Fig. 1B). We examined proliferation activity by measuring BrdU incorporation of CNCCs from multiple colonies. Approximately 70% of cultured CNCCs were positive for BrdU incorporation, a level of proliferation activity that is higher than that of BMMSCs in the identical culture conditions (Fig. 1C).

Next, we examined the expression of MSC markers in postmigratory CNCCs using flow cytometry analysis. Postmigratory CNCCs expressed MSC markers including Sca-1, CD44, CD29, CD90.2, and SSEA4 (supporting information Fig. 1C). We detected almost no expression of CD49e, CD13 (data not shown), CD18, c-Kit, and OCT4. We detected no significant changes to this pattern of marker expression in cultured primary (P0, supporting information Fig. 1C) and subcultured (P1) CNCC. Some of CNCCs were positive both for SSEA4 and other MSC markers including CD29, CD90.2, and Sca-1 (supporting information Fig. 1D). The expression of many MSC markers was comparable in both postmigratory CNCC and BMMSC populations. We detected the greatest variation in the expression of CD90.2 and SSEA4 (elevated in CNCCs) and CD18 (absent in CNCCs; Fig. 1D).

## Multipotent Differentiation of Postmigratory CNCCs

The multiple differentiation potentials of the CNCCs to undergo osteogenesis, adipogenesis, and chondrogenesis were examined. Initially, we promoted osteogenic differentiation of cultured postmigratory CNCC by switching to osteogenic induction medium. After 2 weeks of osteogenic induction, alkaline phosphatase (Fig. 2A) expression was elevated, and after 6 weeks calcified nodule formation was detectable after alizarin red staining (Fig. 2B). When we compared the expression intensity of these markers, we found that expression was higher in CNCCs. In addition, the internal calcium concentration was higher in CNCCs than in BMMSCs.

Next, we examined adipogenic induction of cultured postmigratory CNCCs. We found that some of the CNCCs were positive for lipid production, based on Oil Red O staining after 2 weeks of culture in adipogenic media (Fig. 2C). CNCCs in adipogenic media expressed an elevated level of adipogenic markers including peroxisome proliferator-activated receptor gamma 2 and lipoprotein lipase. The number of cells showing lipid droplets of CNCCs in each well was comparable to that of BMMSCs (Fig. 2D). In addition, we assessed chondrogenic differentiation after induction in chondrogenic medium by immunostaining for type II collagen expression and by using toluidine blue staining to detect the proteoglycan-rich extracellular matrix (Fig. 2E). Expression of these chondrogenic markers was similar in CNCCs and BMMSCs 4 weeks following induction. On the basis of these findings, we conclude that postmigratory CNCCs, like MSCs, possess intrinsic multidifferentiation ability.

To determine the multidifferentiation potential of postmigratory CNCCs in vivo, we mixed CNCCs with HA/TCP ceramic powder to transplant subcutaneously into immunocompromised mice [20,23]. After 8 weeks, we observed bone formation. The newly formed bone showed characteristic features of craniofacial bone, which contained lamella structures and few hematopoietic components, and were separated by connective tissues (Fig. 2Fa). After X-gal staining (Fig. 2Fb, 2Fc, 2Fe, 2Ff), the osteocytes appeared blue, indicating that postmigratory CNCCs differentiated into osteoblasts and formed bone matrix. Alizarin red and von Kossa staining were consistent with bone matrix formation (Fig. 2Fd, 2Fg). The expression of osteogenic makers such as alkaline phosphatase and osteocalcin was elevated along the periphery of the HA/TCP (Fig. 2Fh, 2Fi). This area corresponded with the lacZ-positive area

(Fig. 2Fe). This expression pattern of osteogenic markers and $\beta$-galactosidase activity indicates that the osteogenic fronts originated from transplanted CNCCs. Thus, we conclude that postmigratory CNCCs can form bone matrix.

To evaluate the role of carrier vehicle on the differentiation of transplanted CNCCs, we transplanted CNCCs with Matrigel and Gelfoam. Eight weeks after transplantation, we detected CNCCs in transplants, but we were unable to detect bone formation in either experimental sample. The CNCCs transplanted with Matrigel contributed to tendon-like structures (Fig. 2Ga, 2Gc). The tendon-like structures were contained in collagen matrix based on picrosirius red and Masson's trichrome staining (Fig. 2Ge, 2Gg). The CNCCs transplanted with Gelfoam produced a fibrous tissue mass (Fig. 2Gb, 2Gd). After staining with picrosirius red and Masson's trichrome (Fig. 2Gf, 2Gh), we found that CNCCs transplanted with Gelfoam are also capable of forming condensed collagen matrix. On the basis of this data, we conclude that HA/TCP is the best choice for the osteogenic carrier, compared with Matrigel and Gelfoam. In addition, these transplantation experiments have confirmed that postmigratory CNCCs are capable of differentiating into specific types of tissues under the influence of specific environmental conditions.

## Postmigratory CNCCs Are Self-Renewing

Self-renewal is a hallmark of stem cells. To evaluate self-renewal, we examined CNCCs for their colony forming and differentiation potential after serial in vitro and in vivo expansion [21]. Initially, postmigratory CNCCs were isolated, expanded in vitro and then transplanted subcutaneously with HA/TCP. After 4-5 weeks, the transplants were removed, digested and then expanded again in vitro before examination for MSC features (Fig. 3A). The transplant-derived CNCCs retained their ability to form colonies (0.1% ± 0.03%; Fig. 3B), when cultured at a low cell density ($5 \times 10^3$ cells in Ø 10-cm culture dish). Morphologically, the X-gal positive cells showed heterogeneity similar to that of primary cultures. The transplant-derived CNCCs retained their ability to differentiate into osteoblasts and adipocytes (Fig. 3C), and their ability to form bone in vivo when retransplanted with HA/TCP (Fig. 3D).

In addition, we examined the contribution of CNCC-originated cells to the MSCs of the mandible. Cells that originated from the mandible of 7-8-week-old *Wnt1-Cre;R26R* mice can form adherent clonogenic cell clusters. These colony-forming cells were positive for CNCC specific $\beta$-galactosidase after X-gal staining (Fig. 3E). Approximately 90% of the colony forming cells was FDG-positive on FACS analysis. The FDG-positive cells showed elevated expression of MSC markers including Sca-1, CD29, CD44, and CD49e (Fig. 3F). In addition, these CNCC-originated cells have retained their ability to differentiate into osteocytes and adipocytes (Fig. 3G), and form bone when subcutaneously transplanted for 8 weeks with HA/TCP (Fig. 3H). These data demonstrate that even after extended expansion in vitro and in vivo, postmigratory CNCCs retain their clonogenic and multipotent properties and their ability to form bone tissues in vivo, thus confirming their self-renewing potential. In addition, CNCC-originated cells contribute to MSC formation during embryonic development and in adulthood.

## CNCCs Have Distinct Bone-Forming Properties

To characterize bone matrix formation during the regeneration of a craniofacial defect, we transplanted postmigratory CNCCs or BMMSCs into hosts with a calvaria defect (Fig. 4Aa, 4Ab). After transplantation of CNCCs and HA/TCP, we detected bone formation similar to the host predefect calvaria. The newly formed bone contained X-gal positive osteocytes, suggesting that transplanted CNCCs contributed to the repair of the defect (Fig. 4Ac, 4Ad). After transplantation of BMMSCs and HA/TCP, we observed bone formation connecting the defect area with prominent bone marrow space development (Fig. 4Ae, 4Af). Quantitative analysis indicated that the formation of mineralized matrix was greater in CNCC transplants,

however the formation of bone marrow was greater in BMMSC transplants (Fig. 4B). In combined transplantations of CNCCs and BMMSCs with HA/TCP, the newly formed bone showed characteristic features based on the ratio of each cell type (supporting information Fig. S2).

To evaluate the contribution of signaling molecules to the regulation of osteogenic differentiation of postmigratory CNCCs, we examined the effects of growth factors including BMP2, TGF-$\beta$2, and FGF nine based on previous studies [24-28]. After treatment of postmigratory CNCCs with osteogenic induction media, we detected elevated expression of *Runx2, Osteopontin* (Fig. 4C), and Osteocalcin (Fig. 4D). The addition of BMP2 enhanced these effects. In contrast, Osteocalcin staining was decreased after administration of TGF-$\beta$2 or FGF9 in the osteogenic induction medium. If we added BMP2 following FGF9 treatment, expression of osteocalcin was restored, suggesting that the FGF9-induced osteogenic inhibitory effect was reversible (Fig. 4D).

Next, to explore the effects of growth factors on the formation of bone matrix, we transplanted BMP2, TGF-$\beta$2, or FGF9 beads with pellets of HA/TCP and postmigratory CNCCs subcutaneously. In transplanted samples with BMP2 beads, we detected bone marrow and increased deposition of bone. Using immunohistochemistry, we detected CD45-positive bone marrow (Fig. 4E). Thus, we conclude that the concerted action of BMP2 and CNCCs promoted formation of bone marrow along with bone deposition. In transplanted samples with TGF-$\beta$2 beads, we were unable to detect bone matrix and only found fibrous tissues mainly composed of collagen fibers (Fig. 4F). This result is consistent with that from our in vitro experiment, in which we found an inhibitory effect of the TGF-$\beta$ pathway on osteogenic differentiation of CNCCs. Finally, in transplanted samples with FGF9 beads, we found abundant blood vessel formation in areas adjacent to the FGF9 beads, but bone matrix formation was not prominent (Fig. 4G).

## Functional Significance of TGF-$\beta$ Signaling in Regulating Postmigratory CNCCs

To investigate the requirement of TGF-$\beta$ signaling in regulating proliferation and differentiation of postmigratory CNCCs, we dissected the first branchial arch of *Tgfbr2*$^{fl/fl}$*;R26R;Wnt1-Cre* mice and cultured postmigratory CNCCs. We found that the cell morphology of *Tgfbr2*-mutant (*Tgfbr2*$^{fl/fl}$*;Wnt1-Cre*) and heterozygous (*Tgfbr2*$^{fl/+}$*;Wnt1-Cre*) CNCC cultures were almost indistinguishable initially. Over time, however, *Tgfbr2*$^{fl/fl}$*;Wnt1-Cre* CNC cells exhibited higher proliferation activity and reached confluence more rapidly than did the heterozygous control sample (Fig. 5A). We performed BrdU incorporation analyses and found that the level of incorporation in *Tgfbr2*$^{fl/fl}$*;Wnt1-Cre* CNCCs was elevated compared to that of the heterozygote (Fig. 5B). To explore the effect of TGF-$\beta$ signaling on the stem cell characteristics of CNCCs, we examined MSC markers as described earlier. The CNCCs from both *Tgfbr2*$^{fl/fl}$*;Wnt1-Cre* and *Tgfbr2*$^{fl/+}$*;Wnt1-Cre* mice expressed *S*ca-1, CD44, CD29, CD90.2, and SSEA4 as we previously observed in *Wnt1-Cre;R26R* CNCCs (Figs. 1F, 5C). The expression levels of *S*ca-1, CD44, and SSEA4 were higher in *Tgfbr2*$^{fl/fl}$*;Wnt1-Cre* CNCCs than in heterozygous control CNCCs. In contrast, the expression level of CD49e was lower in *Tgfbr2*$^{fl/fl}$*;Wnt1-Cre* CNCCs (Fig. 5C).

Next, we examined the requirement for TGF-$\beta$ signaling in osteogenic differentiation. Following 2 weeks of osteogenic induction, CNCCs from *Tgfbr2*$^{fl/fl}$*;Wnt1-Cre* mice expressed an elevated level of *Runx2* and alkaline phosphatase. Moreover, the expression level of *Runx2* after osteogenic induction was higher in postmigratory CNCCs from *Tgfbr2*$^{fl/fl}$*;Wnt1-Cre* than in the heterozygous control (Fig. 5D). At 8 weeks post-transplantation with HA/TCP, CNCCs from *Tgfbr2*$^{flfl}$*;Wnt1-Cre*, as well as heterozygous control, samples formed bone matrix (Fig. 5E). On the basis of these results, we conclude that TGF-$\beta$ signaling has an inhibitory effect on the proliferation and osteogenic differentiation of postmigratory CNCCs.

## Postmigratory CNCCs Support Tooth Germ Survival

To investigate the role of CNCCs in the development of tooth germs, we transplanted developing tooth germs with cultured CNCCs and HA/TCP subcutaneously into the dorsal surface of immunocompromised mice. When tooth germs were transplanted with HA/TCP ($n$ = 18), we detected no tooth development. A few tooth germs cultured without CNCCs gave rise to keratinized cysts instead of normal dental structures (Fig. 6A). In most cases, intramembranous bone formed without tooth development (Fig. 6B), and the transplanted tooth germs showed osteo-inductive potential as previously reported [29].

The transplantation of tooth germs with CNCCs and HA/TCP resulted in apparently normal tooth formation, including crown (Fig. 6C, 6D), root (Fig. 6E), and supporting structures such as periodontal ligament and alveolar bone (Fig. 6E, 6F). After X-gal staining, we visualized transplanted CNCCs within dental pulp tissues (Fig. 6D) and alveolar bone around the tooth (Fig. 6F). We were unable to detect transplanted CNCCs in the dentin and enamel matrix, suggesting that these calcified dental structures originated solely from the transplanted tooth germs. We used tartrate-resistant acid phosphatase (TRAP) staining to detect endogenous $\beta$-galactosidase activities by osteoclasts and found TRAP-positive cells in the bone marrow space and blood vessels (Fig. 6G). The X-gal positive cells in the dental pulp tissues and alveolar bone were all TRAP-negative. This result suggests that X-gal positive cells originated from transplanted postmigratory CNCCs.

We also transplanted tooth germs from *Wnt1-Cre;R26R* mice (X-gal positive) with BMMSCs from wild-type mice (X-gal negative) using HA/TCP as a carrier. After 8 weeks, most of the transplanted tooth germs gave rise to X-gal positive cyst or bone matrix formation (Fig. 6H), indicating that cells from the transplanted tooth germs differentiated into osteoblasts and formed bone. Of 12 transplanted tooth germs, we only detected two teeth, and they were abnormal with disrupted root and periodontal structures (Fig. 6I). On the basis of this data, we conclude that the role of transplanted CNCCs in tooth development is to contribute to the proper formation of supporting structures and to promote the survival of the tooth germ.

## BMP Signals Play a Crucial Role in CNCC-Mediated Tooth Development

Tooth germs transplanted with growth factors without CNCCs resulted in cyst and bone matrix formation instead of normal dental structures (Fig. 7A–7C). Next, pellets containing tooth germs, HA/TCP, and CNCCs were transplanted together with beads containing BMP4 or the BMP antagonist, Noggin. Application of BMP4 beads into transplants resulted in normal teeth with well-formed periodontal structures (Fig. 7D). In tooth germs transplanted with Noggin beads, however, we found cystic degeneration (Fig. 7D). In 2 of 10 transplanted tooth germs, we did detect abnormal tooth structure development (data not shown).

BMP signaling functions via the Smad proteins, including the central mediator, Smad4 [30]. To gain further insight into the role of BMP signal in CNCC and tooth development, we cultured postmigratory CNCCs from the first branchial arch of *Smad4*$^{fl/fl}$*;R26R;Wnt1-Cre* mice. We examined the survival and differentiation of these cells (supporting information Fig. 3), and transplanted them with tooth germs ($n$ = 5) and HA/TCP. The transplanted tooth germs gave rise to intramemebranous bone formation and cysts (Fig. 7E). In parallel, we inhibited the expression of *Smad4* in postmigratory CNCCs using siRNA treatment. When the siRNA-treated CNCCs were transplanted with tooth germs and HA/TCP, the tooth germs produced malformed teeth or cystic degeneration (Fig. 7F). Taken together, these results suggest that postmigratory CNCCs support tooth germ survival in part via BMP signaling in our CNCC-tooth germ cotransplantation system.

Finally, to examine the role of BMP4 in BMMSC-mediated tooth development, we transplanted tooth germs with BMMSCs, HA/TCP, and BMP4 beads. The tooth germs resulted in cystic degeneration and bone matrix formation (Fig. 7G).

Thus, CNCCs have unique properties for tooth development and function to provide signals that promote the survival of developing organs.

## Discussion

Our results demonstrate that postmigratory CNCCs, like MSCs, maintain stem cell characteristics and can differentiate into specific cell and tissue types according to the environmental conditions. Characteristically, CNCCs migrate from their original site and populate the branchial arches for development of craniofacial mesenchymal structures. Our current findings suggest that CNCCs maintain stem cell characteristics during their migration. After arrival at their destination, the fate of CNCCs is determined in part by the interaction of the CNCCs and their microenvironment. Recent studies have shown that stem cells express specific markers [31-33]. We have found that postmigratory CNCCs express elevated level of CD90.2 (Thy 1.2) and SSEA4, in addition to other MSC markers. CD90.2 is a thymus cell antigen and also considered a marker of nerve fibroblasts [31,34]. SSEA4 is expressed by certain neural cells, including the dorsal root ganglion and progenitor cells from the forebrain [35]. These findings are consistent with a neural differentiation potential of postmigratory CNCCs, as we also detected elevated expression of Nestin. Moreover, CD90 and SSEA4 are highly expressed in embryonic stem cell (ESC) lines [36]. Thus, postmigratory CNCCs may be more similar to ESCs than BMMSCs. These findings imply that postmigratory CNCCs are unique stem cell populations, having characteristics of MSCs and ESCs. Furthermore, some of populations of postmigratory CNCC-derived cells retain stem property into adulthood. Interestingly, the expression pattern of some MSC markers changes during development. In mandiblular MSCs, the expression level of CD90.2 and SSEA4 was decreased, and that of CD29, CD44, Sca-1, and CD49e was increased, compared with embryonic stage MSCs. Thus, properties of CNCC-originated stem cells change during their contribution to the development of craniofacial structures.

Postmigratory CNCCs are apparently more responsive to in vitro osteogenic induction than BMMSCs, consistent with the previous result that neural crest-derived progenitor cells showed increased osteogenic capacity and enhanced osteogenisis compared with mesoderm-derived progenitor cells [37]. In addition, following transplantation into hosts, CNCCs formed bone with densely packed lamella structures that were separated by abundant connective tissues. Unlike bone originating from BMMSCs, CNCC-derived bone did not contain prominent hematopoietic components. These features are characteristic of craniofacial bone from intramembranous ossifications. The differences in the histological appearance of bone formed by postmigratory CNCCs and BMMSCs may relate to the differences in embryological origin and functional demands at each skeletal site [38]. The long bones are physiologically adapted for the support of body weight, contain more bone marrow, and contribute more to hematopoiesis [39]. In contrast, CNCC-originated mandible and maxilla are parts of the craniofacial complex, contain less bone marrow, but offer protection for vital structures including paranasal sinuses, dentition, and neurovascular bundles [38]. Skeletal bone formation results from endochondral ossification, in which hypertrophic chondrocytes mineralize their surrounding matrix and attract blood vessels. Consequently, long bones contain more abundant bone marrow than craniofacial bones. The proper formation of bone marrow requires the normal development of skeletal bones. Several studies of mutant mice, in which hematopoiesis is defective as a consequence of primary defects in bone development, have implicated osteoblasts in the formation and function of the bone marrow hematopoietic stem cell environment [40]. In addition, cells involved in bone formation play a role supporting the

development of hematopoietic component, and specialized osteoblasts lining the bone marrow function to maintain and regulate hematopoietic stem cells [40]. During endochondral ossification, hypertrophic chondrocytes express BMP2 and BMP6, and deficiency of *Bmp2* and *Bmp6* in mice results in a reduction of trabecular bone volume with suppressed bone formation [25,41]. When we added BMP2 into the transplants of CNCC and HA/TCP, we observed increased bone marrow along with increased bone formation. Thus, the concerted action of BMP2 and CNCCs resulted in increased formation of hematopoietic components in the bone matrix, consistent with the previous study showing that bone marrow development in rat mandible occurred in a BMP2 dose-dependent fashion [42]. Administration of BMP2 to postmigratory CNCCs caused expression of some morphological features of skeletal bone formation. Thus, the microenvironment may influence how postmigratory CNCCs can differentiate and regenerate tissues.

Conventionally, developing tooth germs have been transplanted into kidney capsules to evaluate their development and the effect of signaling factors. Underneath the kidney capsule, the transplanted tooth germs receive a sufficient nutritional supply to develop to mature stages. In contrast, we transplanted tooth germs subcutaneously into immunocompromised mice to evaluate the role of stem cells and growth factors on the survival of tooth organs without the interfering effect of host nutritional supply. Following the subcutaneous transplantation of tooth germs and postmigratory CNCCs, we detect apparently normal tooth development. Because we are able to detect transplanted CNCCs in the supporting structures including dental pulp and bone adjacent to the tooth, we conclude that postmigratory CNCCs are a key factor for tooth germ survival. In addition, well-formed supporting structures, especially the alveolar bone, are required for the proper development of teeth. In the transplants of BMMSC and tooth germs we failed to detect normal tooth, likely due to the abnormal supporting structures. Thus, it appears that CNCC-originated bone, with its features of craniofacial bone, is required for the survival of tooth germs. Differences in supporting structures based on the embryonic origin between CNCCs and BMMSCs may explain the abnormal tooth development in BMMSC-tooth transplants.

Various transcription factors and signaling molecules including BMP, FGF, Activin, Hedgehog, and Wnt family members participate in tooth development [43,44]. Among these, BMPs are believed to be key signals [44-46]. In loss-of-function studies that inhibit BMP activity using Noggin, subrenal transplantation of Noggin-treated tooth germs gave rise to keratinized cysts [15]. In addition, during jaw bone development, BMP activity plays a vital role in the formation of alveolar bone via a *Bmp/Msx* signaling cascade [15,47,48]. In *Msx1*$^{-/-}$ mice, tooth development is arrested at the bud stage and the alveolar bone is absent. Ectopic expression of *Bmp4* driven by the mouse *Msx1* promoter in *Msx1*$^{-/-}$ dental mesenchyme not only partially restores tooth development, but it also rescues alveolar bone formation [48]. These studies are consistent with our findings that inhibition of BMP signal using Noggin beads or inactivation of Smad4 in CNCCs resulted in abnormal tooth development in tooth germ transplants. However, administration of BMP4 into the transplants of BMMSCs and tooth germs failed to promote normal tooth development. This result suggests that BMP signaling in CNCCs is required, but not sufficient, to support tooth formation. There is an intrinsic difference between CNCCs and BMMSCs in tooth development and postmigratory CNCCs have unique properties important for tooth development. Postmigratory CNCCs link alveolar bone and tooth development as a functional unit, and these cells have an ability to support organ survival environment—defined as an “organ niche,” which can provide proper niche condition for tooth germ survival.

## Conclusion

We report the novel identification of postmigratory CNCCs as a population of stem cells having characteristics of MSCs. BMP and TGF-$\beta$ signaling controls the differentiation and fate of postmigratory CNCCs, and postmigratory CNCCs support ectopic tooth germ survival and development via BMP signaling. Moreover, transplanted CNCCs can mediate the proper development of alveolar bone and tooth as a functional unit. These findings offer new opportunities for studying the role of postmigratory CNCCs in craniofacial development and for designing a biological solution to regenerate craniofacial structures.

## Acknowledgments

We thank Dr. Julie Mayo and Dr. Gage Crump for critical reading of the manuscript. This study was supported by grants from the National Institute of Dental and Craniofacial Research, NIH (DE012711, DE014078, DE017007) to Yang Chai.

## References

1. Noden DM. Cell movements and control of patterned tissue assembly during craniofacial development. J Craniofac Genet Dev Biol 1991;11:192–213. [PubMed: 1812125]
2. Le Douarin NM, Ziller C, Coul G. Patterning of neural crest derivatives in the avian embryo: In vivo and in vitro studies. Dev Biol 1993;159:24–49. [PubMed: 8365563]
3. Trainor PA, Krumlauf R. Patterning the cranial neural crest: hindbrain segmentation and Hox gene plasticity. Nat Rev Nurosci 2000;1:116–124.
4. Chai Y, Jiang X, Ito Y, et al. Fate of the mammalian cranial neural crest during tooth and mandibular morphogenesis. Development 2000;127:1671–1679. [PubMed: 10725243]
5. Chai Y, Maxson RE Jr. Recent advances in craniofacial morphogenesis. Dev Dyn 2006;235:2353–2375. [PubMed: 16680722]
6. Le Douarin NM, Dupin E. Multipotentiality of the neural crest. Curr Opin Genet Dev 2003;13:529–536. [PubMed: 14550420]
7. Graham A, Begbie J, McGonnell I. Significance of the cranial neural crest. Dev Dyn 2004;229:5–13. [PubMed: 14699573]
8. Bronner-Fraser M, Fraser SE. Cell lineage analysis reveals multipotency of some avian neural crest cells. Nature 1988;335:161–164. [PubMed: 2457813]
9. Fraser S, Bronner-Fraser M. Migrating neural crest cells in the trunk of the avian embryo are multipotent. Development 1991;112:913–920. [PubMed: 1935700]
10. Stemple DL, Anderson DJ. Isolation of a stem cell for neurons and glia from the mammalian neural crest. Cell 1992;71:73–985. [PubMed: 1327537]
11. Le Douarin NM, Creuzet S, Couly G, et al. Neural crest cell plasticity and its limits. Development 2004;131:4637–4650. [PubMed: 15358668]
12. Lo L, Anderson DJ. Postmigratory neural crest cells expressing c-RET display restricted developmental and proliferative capacities. Neuron 1995;15:527–539. [PubMed: 7546733]
13. Sieber-Blum M, Ito K, Richardson MK, et al. Distribution of pluripotent neural crest cells in the embryo and the role of brain-derived neurotrophic factor in the commitment to the primary sensory neuron lineage. J Neurobiol 1993;24:173–184. [PubMed: 8445386]
14. Sodek J, McKee MD. Molecular and cellular biology of alveolar bone. Periodontol 2000;24:99–126.
15. Zhang Z, Song Y, Zhang X, et al. Msx1/Bmp4 genetic pathway regulates mammalian alveolar bone formation via induction of Dlx5 and Cbfa1. Mech Dev 2003;120:1469–1479. [PubMed: 14654219]
16. Zhao H, Bringas P Jr, Chai Y. An in vitro model for characterizing the post-migratory cranial neural crest cells of the first branchial arch. Dev Dyn 2006;235:433–1440.
17. Danielian PS, Muccino D, Rowitch DH, et al. Modification of gene activity in mouse embryos in utero by a tamoxifen-inducible form of Cre recombinase. Curr Biol 1998;8:1323–1326. [PubMed: 9843687]

18. Soriano P. Generalized *lac* Z expression with the ROSA26 Cre reporter strain. Nat Genet 1999;21:70–71. [PubMed: 9916792]
19. Sasaki T, Ito Y, Bringas P Jr, et al. TGF$\beta$-mediated Fgf signaling is crucial for regulating cranial neural crest cell proliferation during frontal bone development. Development 2006;133:371–381. [PubMed: 16368934]
20. Ko SO, Chung IH, Xu X, et al. Smad4 is required to regulate the fate of cranial neural crest cells. Dev Biol 2007;31:435–447. [PubMed: 17964566]
21. Bi Y, Ehirchiou D, Kilts TM, et al. Identification of tendon stem/progenitor cells and the role of the extracellular matrix in their niche. Nat Med 2007;13:1219–1227. [PubMed: 17828274]
22. Oka K, Oka S, Sasaki T, et al. The role of TGF-$\beta$ signaling in regulating chondrogenesis and osteogeneisis during mandibular development. Dev Biol 2007;303:391–404. [PubMed: 17204263]
23. Ohgushi H, Caplan AI. Stem cell technology and bioceramics: From cell to gene engineering. J Biomed Mater Res (Appl Biomater) 1999;48:913–927.
24. Yamaguchi A, Katagiri T, Ikeda T, et al. Recombinant human bone morphogenetic protein-2 stimulates osteoblastic maturation and inhibits myogenic differentiation in vitro. J Cell Biol 1991;113:681–687. [PubMed: 1849907]
25. Kugimiya F, Kawaguchi H, Kamekura S, et al. Involvement of endogenous bone morphogenetic protein (BMP) 2 and BMP6 in bone formation. J Biol Chem 2005;280:35704–35712. [PubMed: 16109715]
26. Ryoo HM, Lee MH, Kim YJ. Critical molecular switches involved in BMP-2-induced osteogenic differentiation of mesenchymal cells. Gene 2006;366:51–57. [PubMed: 16314053]
27. Shen ZJ, Kim SK, Jun DY, et al. Antisense targeting of TGF-$\beta$1 augments BMP induced upregulation of osteopontin, type 1 collagen and cbfa1 in human Saos-2 cells. Exp Cell Res 2007;313:1415–1425. [PubMed: 17359969]
28. Fakhry A, Ratisoontorn C, Vedhachalam C, et al. Effects of FGF-2/-9 in calvarial bone cell cultures: Differentiation stage-dependent mitogenic effect, inverse regulation of BMP-2 and noggin, and enhancement of osteogenic potential. Bone 2005;36:254–266. [PubMed: 15780951]
29. Kim JY, Cho SW, Hwang HJ, et al. Evidence for expansion-based temporal BMP4/NOGGIN interactions in specifying peridontium morphogenesis. Cell Tissue Res 2007;330:123–132. [PubMed: 17618464]
30. Massague J, Blain SW, Lo RS. TGF beta signaling in growth control, cancer, and heritable disorders. Cell 2000;103:295–309. [PubMed: 11057902]
31. da Silva Meirellis L, Chagastelles PC, Nardi NB. Mesechymal stem cells reside in virtually all post-natal organs and tissues. J Cell Sci 2006;119:2204–2213. [PubMed: 16684817]
32. Kolf CM, Cho E, Tuan RS. Biology of adult mesenchymal stem cells: Regulation of niche, self-renewal and differentiation. Arthritis Res Ther 2007;9:204–213. [PubMed: 17316462]
33. Owens GK. Regulation of differentiation of vascular smooth muscle cells. Physiol Rev 1995;75:487–517. [PubMed: 7624392]
34. Joseph N, Mukouyama Y, Mosher J, et al. Neural crest stem cells undergo multilineage differentiation in developing peripheral nerves to generate endoneurial fibroblasts in addition to Schwann cells. Development 2004;131:5599–5612. [PubMed: 15496445]
35. Barraud P, Stott S, Mollgard K, et al. In vitro characterization of a human neural progenitor cell coexpressing SSEA4 and CD133. J Neurosci Res 2007;85:250–259. [PubMed: 17131412]
36. The International Stem Cell Initiative. Adewumi O, Aflatoonian B, Ahrlund-Richter L, et al. Characterization of human embryonic stem cell lines by the international stem cell initiative. Nat Biotechnol 2007;25:803–816. [PubMed: 17572666]
37. Leucht P, Kim JB, Amasha R, et al. Embryonic origin and Hox status determine progenitor cell fate during adult bone regeneration. Development 2008;135:2845–2854. [PubMed: 18653558]
38. Akintoye S, Lam T, Shi S, et al. Skeletal site-specific characterization of orofacial and iliac crest human bone marrow stromal cells in same individuals. Bone 2006;38:758–768. [PubMed: 16403496]
39. Charbord P, Tavian M, Humeau L, et al. Early ontogeny of the human marrow from long bones: An immunohistochemical study of hematopoiesis and its microenvironment. Blood 1996;87:4109–4119. [PubMed: 8639768]

40. Wilson A, Trumpp A. Bone-marrow haematopoietic-stem-cell niches. Nat Rev Immunol 2006;6:93–106. [PubMed: 16491134]

41. Chung UI, Schipani E, McMahon AP, et al. Indian hedgehog couples chondrogenesis to osteogenesis in endochondral bone development. J Clin Invest 2001;107:295–304. [PubMed: 11160153]

42. Arosarena O, Collins W. Comparison of BMP-2 and -4 for rat mandibular bone regeneration at various doses. Orthod Craniofac Res 2005;8:267–276. [PubMed: 16238607]

43. Peters H, Balling R. Teeth where and how to make them. Trends Genet 1999;15:59–65. [PubMed: 10098408]

44. Thesleff I, Sharpe P. Signaling networks regulating dental development. Mech Dev 1997;67:111–123. [PubMed: 9392510]

45. Vainio S, Karavanova I, Jowett A, et al. Identification of BMP-4 as a signal mediating secondary induction between epithelial and mesenchymal tissues during early tooth development. Cell 1993;75:45–58. [PubMed: 8104708]

46. Plikus MV, Zeichner-David M, Mayer JA, et al. Morphoregulation of teeth: Modulating the number, size, shape and differentiation by tuning Bmp activity. Evol Dev 2005;7:440–457. [PubMed: 16174037]

47. Nie X, Luukko K, Kettunen P. BMP signaling in craniofacial development. Int J Dev Biol 2006;50:511–521. [PubMed: 16741866]

48. Zhao X, Zhang Z, Song Y, et al. Transgenically ectopic expression of Bmp4 to the Msx1 mutant dental mesenchyme restores downstream gene expression but represses Shh and Bmp2 in the enamel knot of wild type tooth germ. Mech Dev 2000;99:29–38. [PubMed: 11091071]

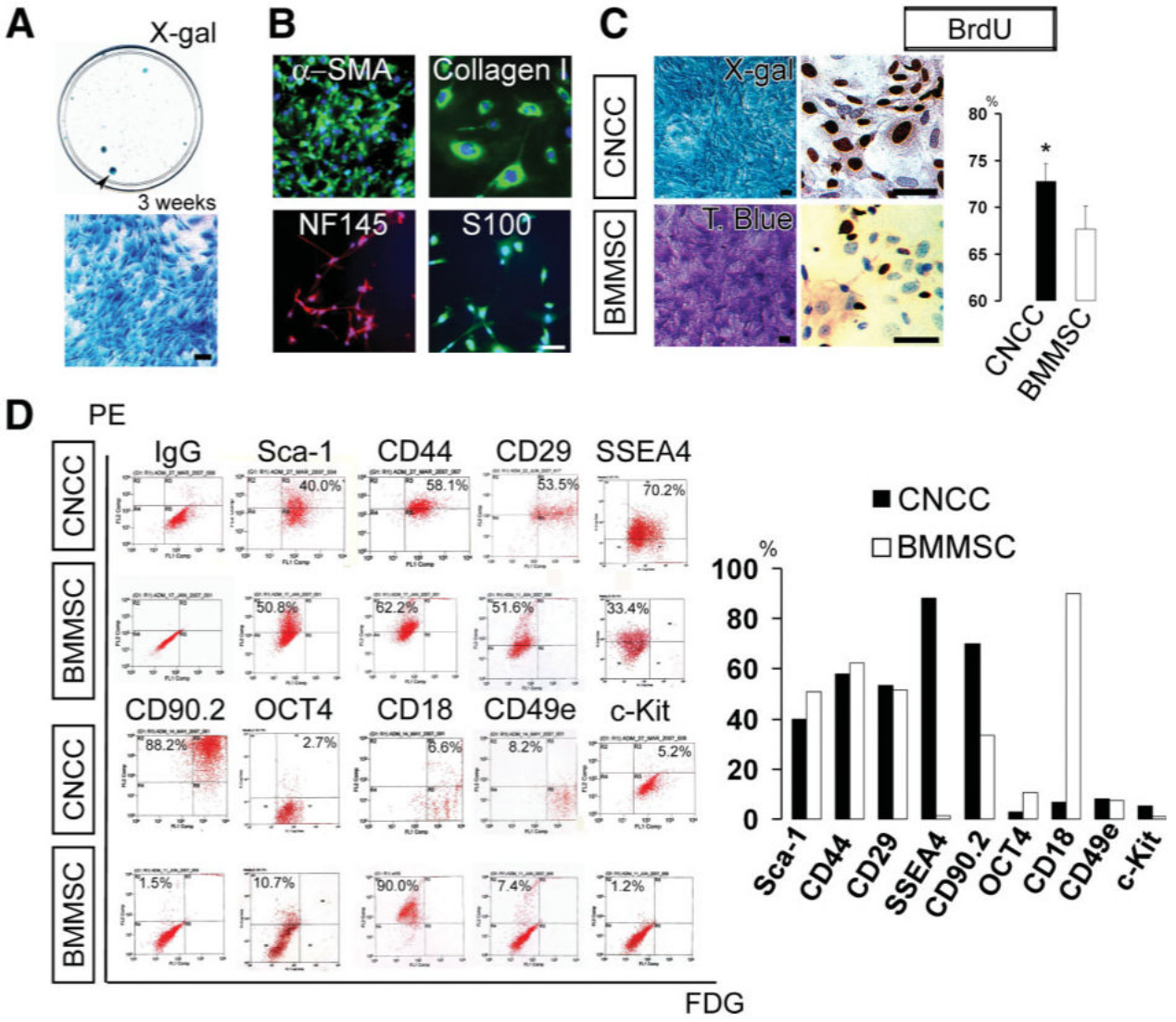


**Figure 1.**

Stem cell characteristics of postmigratory CNCCs. **(A):** Postmigratory CNCCs cultured at a low cell density ($5 \times 10^3$ cells in Ø 10-cm culture dish) for 3 weeks formed adherent clonogenic cell clusters (arrow head), visualized with X-gal staining. Top: The culture dish with several X-gal+ colonies. Arrowhead indicates a colony. Bottom: Magnified image of an X-gal+ colony. **(B):** Immunostaining of colonies with $\alpha$-SMA, Type I collagen, NF145, and S100. **(C):** BrdU incorporation assay of multicolony-derived CNCCs and BMMSCs. Right: Quantitation of BrdU incorporation in CNCCs and BMMSCs (*, $p < .05$). **(D):** Fluorescence-activated cell sorting (FACS) analysis of P1 postmigratory CNCC and BMMSC cultures. Right: Quantitation of FACS analysis. Scale bars = 100 $\mu$m **(A, B)**, 50 $\mu$m **(C)**. Abbreviations: BMMSCs, bone marrow mesenchymal stem cells; BrdU, 5-bromo-2prime-deoxyurine; CNCCs, cranial neural crest cells; FDG, fluorescein di-$\beta$-D-galactopyranoside; NF145, neurofilament 145; PE, phycoerythrin; Sca-1, stem cell antigen-1; $\alpha$-SMA, $\alpha$-smooth muscle actin; SSEA4, stage-specific embryonic antigen 4; T Blue, toluidine blue.

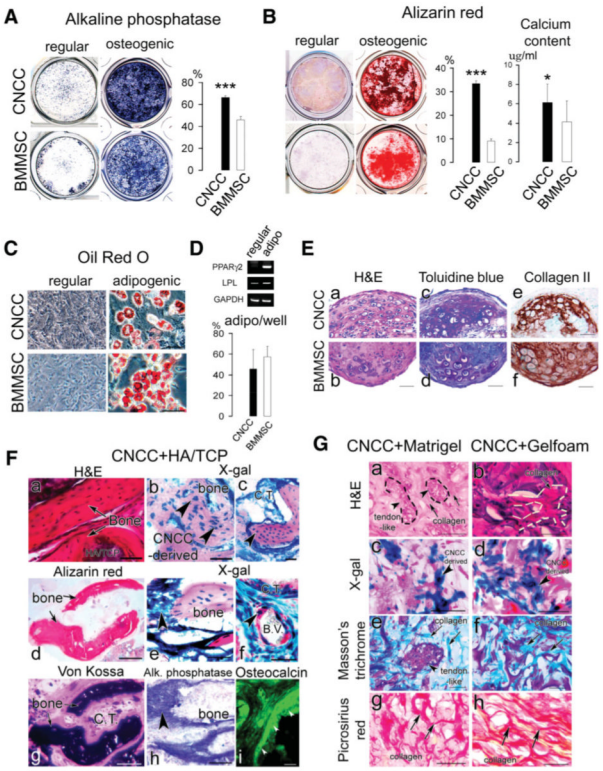


**Figure 2.**

Multipotent differentiation of postmigratory CNCCs. **(A, B):** Osteogenic differentiation of postmigratory CNCCs and BMMSCs. Alkaline phosphatase **(A)** and alizarin red **(B)** analysis of CNCCs and BMMSCs following culture in regular or osteogenic induction medium. Quantitation indicates elevated expression of alkaline phosphatase **(A)** and calcified nodule **(B)** formation in CNCCs following osteogenic induction (***, $p < .001$), and increased calcium concentration (**B**, * , $p < .05$). **(C, D):** Adipogenic differentiation of CNCCs and BMMSCs. Oil Red O staining following culture in regular or adipogenic induction medium **(C)**. Reverse transcription polymerase chain reaction of adipogenic markers PPAR$\gamma$2 and LPL of CNCCs following 2-weeks culture in regular or adipogenic induction medium (**[D]**, top). Quantitation of lipid droplets in CNCCs and BMMSCs (**[D]**, bottom). **(E):** H&E staining **(a, b)**, toluidine blue staining **(c, d)**, and type II collagen immunostaining **(e, f)** of CNCCs and BMMSCs following 4 weeks chondrogenic differentiation. **(F):** Analysis 8 weeks after subcutaneous transplantation of CNCCs and HA/TCP into immunocompromised mice. Bone matrix was detected with H&E staining **(a)**. The osteocytes located in the bone matrix were positive for $\beta$-galactosidase activity after X-gal staining **(b, c, e)**. Alizarin red **(d)** and von Kossa **(g)** staining and expression of alkaline phosphatase **(h)** and osteocalcin **(i)** indicate bone formation. Black arrow heads **(b, c, e, f)** indicate CNCCs-derived cells. **(E):** H&E **(a, b)**, X-gal **(c, d)**, Masson's trichrome **(e, f)**, and picrosirius red **(g, h)** analysis 8 weeks after transplantation of CNCCs with Matrigel or Gelfoam. The transplants of CNCC and Matrigel resulted in tendon-like structures [**(a)**, arrowheads, dashed line circles] with dense collagen matrix deposition (**[e, g]** arrows). The CNCCs transplanted with Gelfoam also resulted in condensed collagen matrix (**[b, f, h]**, arrows, dashed line). Scale bars = 50 $\mu$m. Abbreviations: BMMSCs, bone marrow mesenchymal stem cells; B.V., blood vessel; CNCCs, cranial neural crest cells; C.T., connective tissue; HA/TCP, hydroxyapatite/tricalcium phosphate; LPL, lipoprotein lipase; PPAR$\gamma$2, peroxisome proliferator-activated receptor gamma 2.

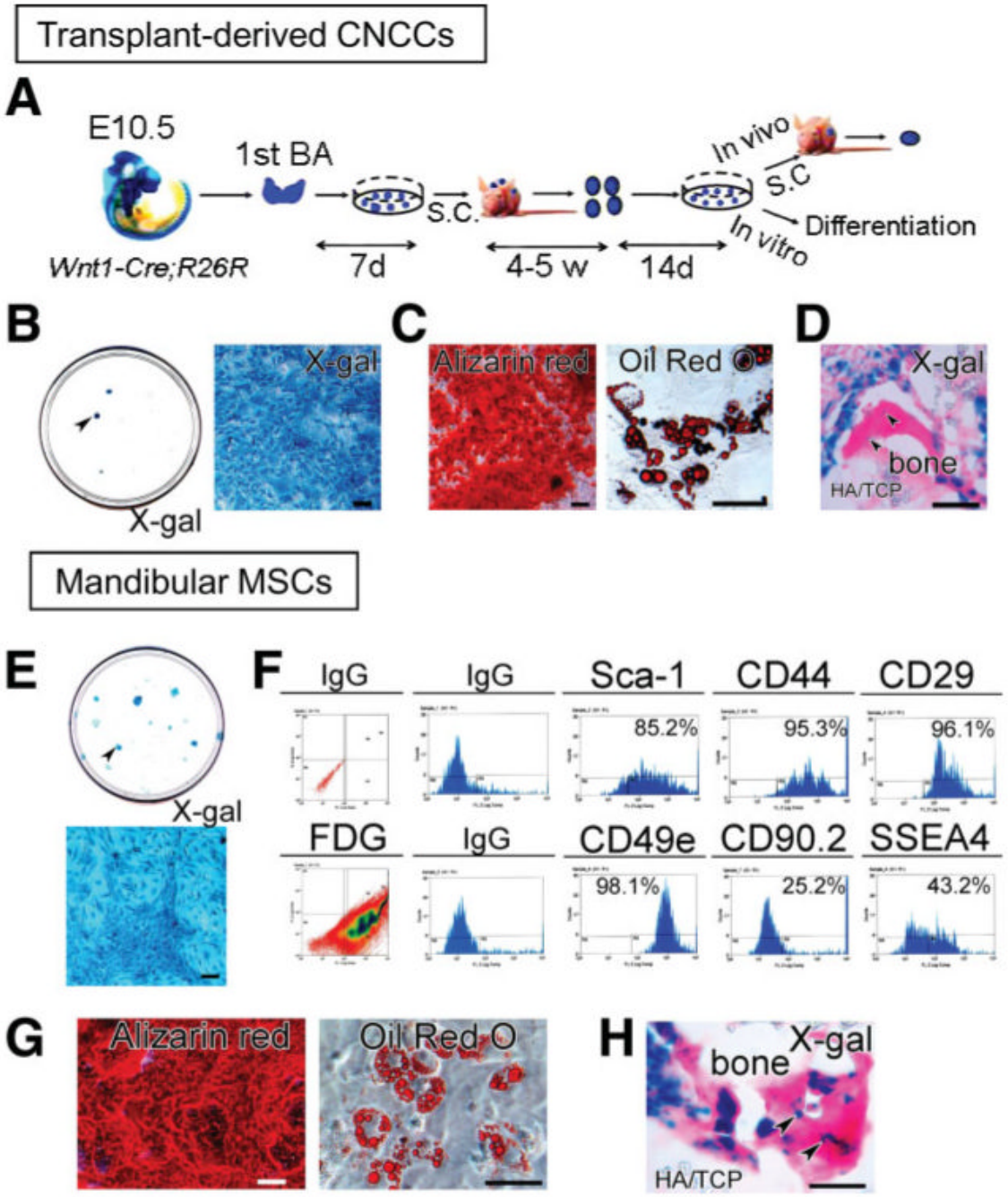


**Figure 3.**

Self-renewal of postmigratory CNCCs. **(A–D):** Transplantderived CNCC cells retain stem cell characteristics. **(A):** Strategy for evaluating self-renewal of postmigratory CNCCs [21]. **(B):** After in vitro and in vivo expansion CNCCs can form colonies (arrow head) when cultured at a low cell density. **(C):** Alizarin red and Oil Red O staining of transplant-derived CNCCs. **(D):** X-gal staining of transplant-derived CNCCs (arrow heads) retransplanted with HA/TCP indicate they retain their ability to form bone in vivo. **(E–H):** The contribution of CNCC-originated cells to the MSCs of the mandible of *Wnt1-Cre;R26R* mice. **(E):** CNCC-originated cells can form clonogenic cell clusters (arrowhead), visualized with X-gal staining. **(F):** Fluorescence-activated cell sorting analysis of CNCC-originated mandibular MSCs. **(G):**

Osteogenic and adipogenic induction of CNCC-originated MSCs, stained with Alizarin red and Oil Red O, respectively. **(H):** CNCC-originated MSCs (arrow heads on X-gal staining) can form bone when subcutaneously transplanted with HA/TCP. Scale bars = 100 $\mu$m **(B, C, E)**, 50 $\mu$m **(D, G, H)**. Abbreviations: BA, branchial arch; CNCCs, cranial neural crest cells; FDG, fluorescein di-$\beta$-D-galactopyranoside; HA/TCP, hydroxyapatite/tricalcium phosphate; MSCs, mesenchymal stem cell; S.C., subcutaneous transplantation; Sca-1, stem cell antigen-1; SSEA4, stage-specific embryonic antigen 4.

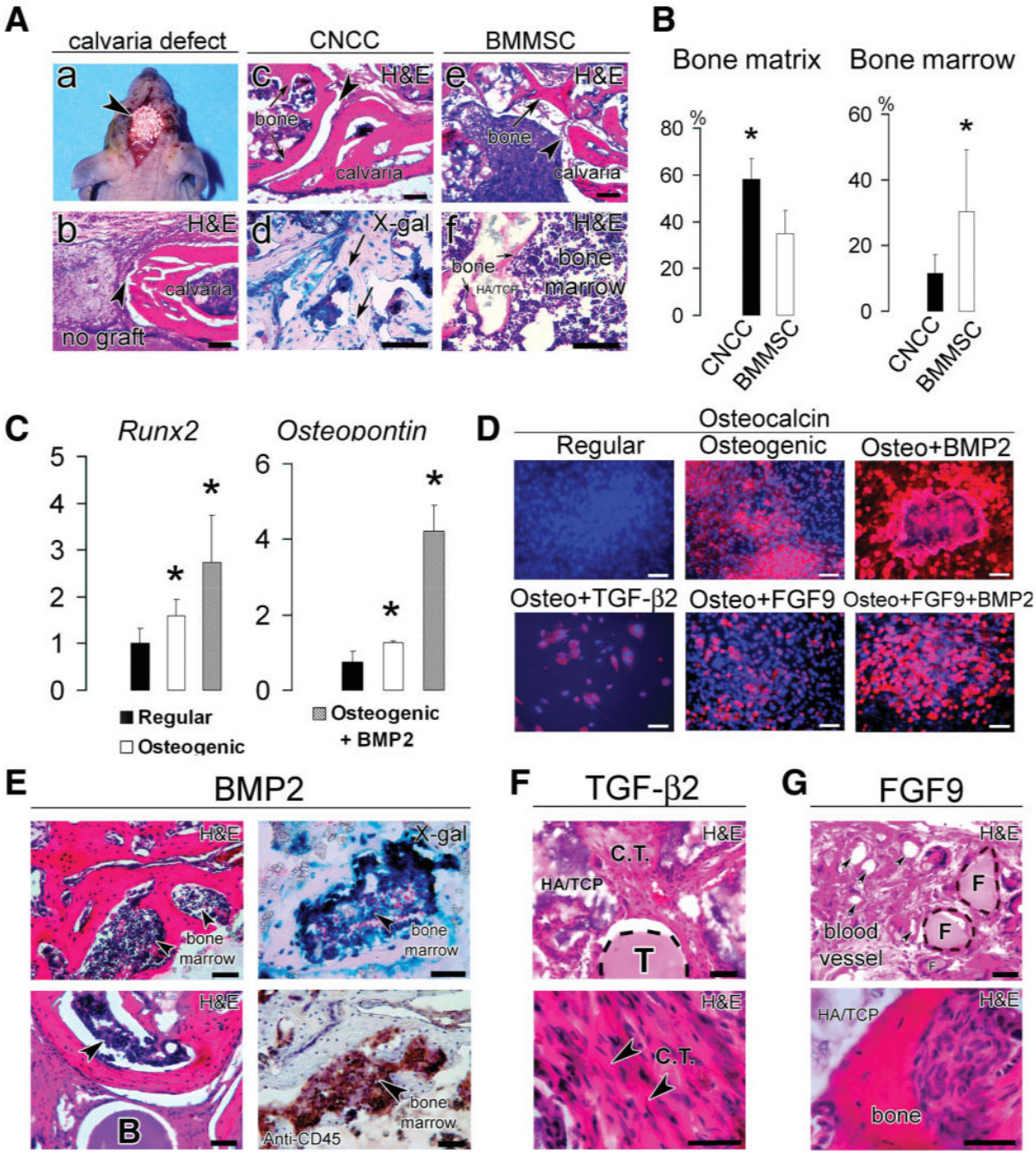


**Figure 4.**

CNCCs have distinct bone-forming properties. **(A, B):** Histological analysis of a defect in the calvaria in mice 8 weeks after transplantation of no graft **(b)**, CNCCs and HA/TCP **(c, d)**, or BMMSCs and HA/TCP **(e, f)**. Arrowheads indicate the margin of the calvarial defect. **(a)** Graft into the calvarial defect. **(b)** No bone formation is detectable by H&E staining in mice that received no graft. **(c, d)** After transplantation of CNCCs and HA/TCP, bone matrix can be detected by H&E staining (arrows) that is similar to the host predefect calvaria **(c)**. The newly formed bone matrix contained X-gal positive osteocytes **(d)**. **(e, f)** Bone can be visualized by H&E staining (arrow) after BMMSCs and HA/TCP transplantation that contains prominent bone marrow space development (f). **(B):** Quantitative analysis indicated that the formation of

mineralized matrix was greater in CNCC transplants (*, $p < .05$), but the formation of bone marrow was greater in BMMSC transplants (*, $p < .05$). **(C):** Quantitative reverse transcription polymerase chain reaction of *Runx2* and *Osteopontin* expression in CNCCs cultured in regular medium, osteogenic induction medium or osteogenic induction medium, and exogenous BMP2. Osteogenic induction medium increased the expression of *Runx2* and *Osteopontin*, and the addition of BMP2 enhanced these effects (*, $p < .05$). **(D):** Immunostaining of Osteocalcin in CNCCs cultured in regular or osteogenic induction medium, alone or with the addition of BMP2, TGF-$\beta$2, or FGF9. **(E):** H&E and X-gal staining and CD45 immunohistochemistry of CNCCs and HA/TCP transplanted with BMP2 beads. Bone marrow space is indicated with arrow heads. **(B):** BMP2. **(F):** H&E staining of transplants with TGF-$\beta$2 beads. Note fibrous tissues (arrow heads) mainly composed of collagen fibers and the absence of bone matrix formation. **(G):** H&E staining of transplants with FGF9 beads. Note small amount of bone matrix and abundant blood vessel formation. **(F):** FGF9 beads. Scale bars = 100 $\mu$m **(D)**, 50 $\mu$m **(A, E–G)**. Abbreviations: BMMSCs, bone marrow mesenchymal stem cells; BMP2, bone morphogenetic protein 2; CNCCs, cranial neural crest cells; C.T., connective tissue; FGF9, fibroblast growth factor 9; HA/TCP, hydroxyapatite/tricalcium phosphate; TGF-$\beta$2, transforming growth factor-$\beta$2.

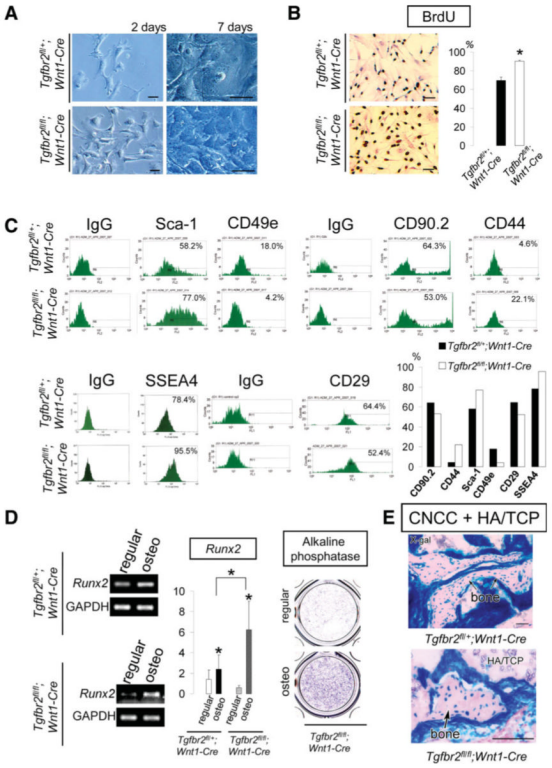


**Figure 5.**

Transforming growth factor-$\beta$ (TGF-$\beta$) signaling regulation of postmigratory CNCCs. **(A):** *Tgfbr2*$^{fl/+}$*;Wnt1-Cre* (control) and *Tgfbr2*$^{fl/fl}$*;Wnt1-Cre* CNCCs after 2 and 7 days of culture. **(B):** BrdU incorporation analysis of *Tgfbr2*$^{fl/+}$*;Wnt1-Cre* (control) and *Tgfbr2*$^{fl/fl}$*;Wnt1-Cre* CNCCs. Statistical analysis indicates that proliferation was higher in CNCCs lacking TGF-$\beta$ (***, $p < .001$). **(C):** Fluorescence-activated cell sorting analysis of *Tgfbr2*$^{fl/+}$*;Wnt1-Cre* (control) and *Tgfbr2*$^{fl/fl}$*;Wnt1-Cre* CNCCs. **(D):** Analysis of osteogenic marker gene expression. Expression of *Runx2*, by reverse transcription polymerase chain reaction, and alkaline phosphatase was assayed in regular and osteogenic induction (osteo) media. Statistical analysis indicates that *Runx2* is elevated in CNCCs lacking TGF-$\beta$ type II receptors (*, $p < .05$). **(E):** Bone matrix formation (arrows) was detected by X-gal staining in *Tgfbr2*$^{fl/+}$*;Wnt1-Cre* (control) and *Tgfbr2*$^{fl/fl}$*;Wnt1-Cre* CNCCs + HA/TCP transplants. Scale bars = 50 $\mu$m. Abbreviations: BrdU, 5-bromo-2′-deoxyurine; BMMSCs, bone marrow mesenchymal stem cells; CNCCs, cranial neural crest cells; HA/TCP, hydroxyapatite/tricalcium phosphate; Sca-1, stem cell antigen-1; SSEA4; stage-specific embryonic antigen 4.

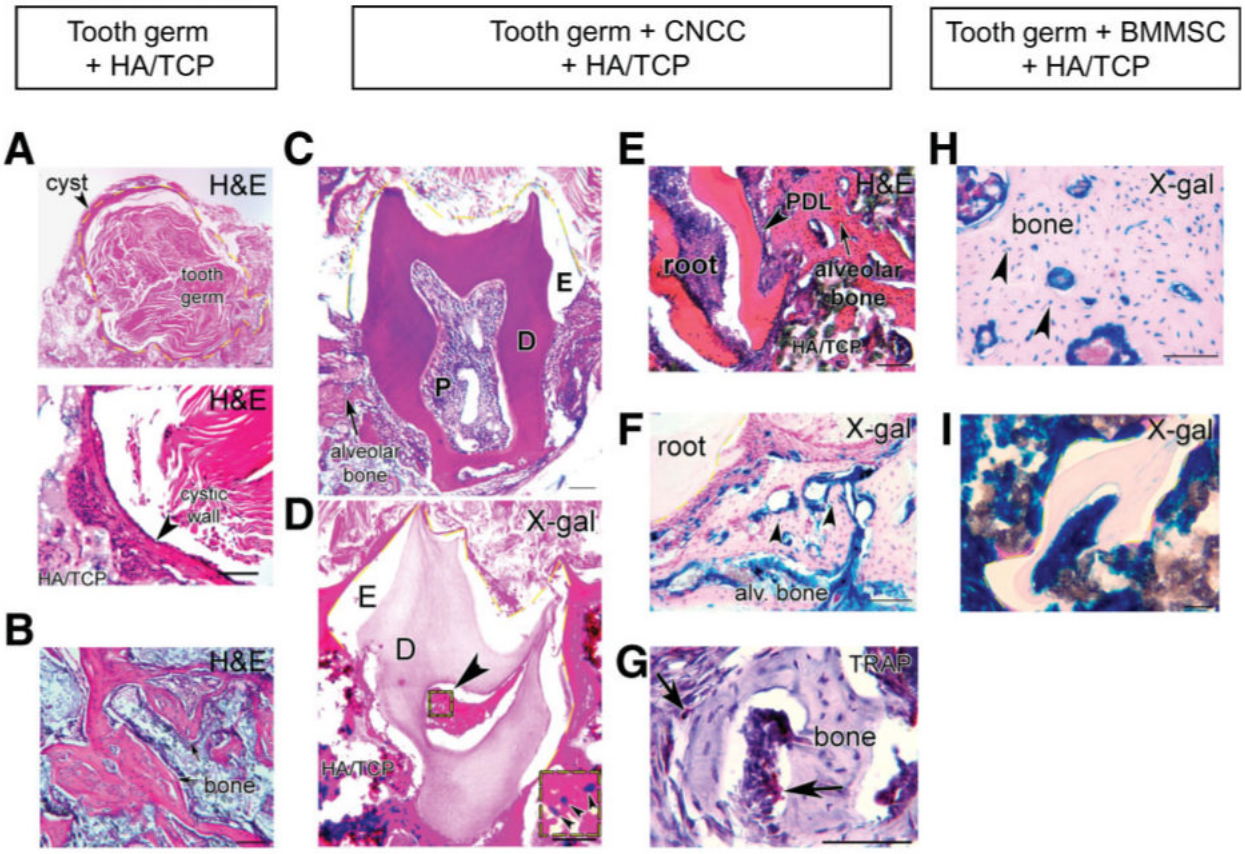


**Figure 6.**

Postmigratory CNCCs support tooth germ survival. Analysis of tooth germs transplanted with HA/TCP alone **(A, B)** or with CNCCs **(C–G)**, or BMMSCs **(H, I)**. **(A, B):** H&E staining indicates that tooth germs transplanted with HA/TCP alone gave rise to keratinized cysts (**[A]**, arrowheads) and intramembranous bone formation (**[B]**, arrows). **(C–G):** H&E **(C)** and X-gal staining **(D)** of tooth germs transplanted with CNCCs and HA/TCP reveal apparently normal teeth. Transplanted CNCCs were detectable within the dental pulp (**[D]**, Lower inset: magnified image, arrow heads) and alveolar bone (**[F]**, arrow heads) after X-gal staining. TRAP-positive staining was present in the bone marrow space and blood vessels (**[G]**, arrows). **(H, I):** Bone matrix formation can be detected by X-gal staining in tooth germs from *Wnt1-Cre;R26R* mice transplanted with BMMSCs and HA/TCP **(H)**. The osteocytes in the bone matrix are positive for $\beta$-galactosidase activity after X-gal staining (**[H]**, arrowheads). Two tooth germs out of twelve transplanted resulted in abnormal tooth formation **(I)**. Scale bars = 50 $\mu$m. Abbreviations: Alv. Bone, alveolar bone; BMMSCs, bone marrow mesenchymal stem cells; CNCCs, cranial neural crest cells; D, dentin; E, enamel; HA/TCP, hydroxyapatite/tricalcium phosphate; P, pulp; PDL, periodontal ligament.

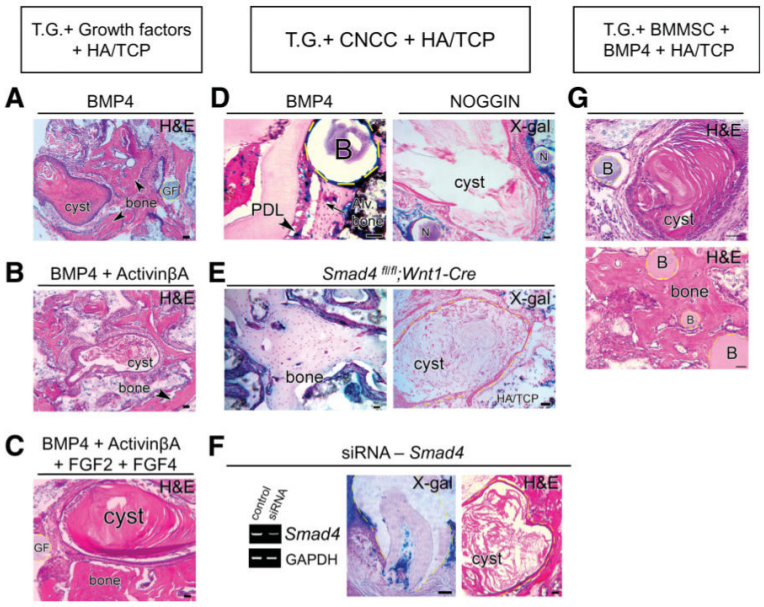


**Figure 7.**

BMP signals play a role in CNCCs-mediated tooth development. **(A–C):** H&E staining of T.G. transplanted with HA/TCP and BMP4 beads **(A)**, BMP4 and Activin*β*A beads **(B)**, or BMP4, Activin*β*A, FGF2, and FGF4 beads **(C)**. The T.G. gave rise to cysts and bone. Arrowheads indicate bone. **(D):** X-gal staining of T.G. transplanted with CNCCs, HA/TCP, and BMP4, or Noggin beads. **(E):** X-gal staining of tooth germs transplanted with CNCCs from *Smad4*$^{fl/fl}$*;Wnt1-Cre* mice and HA/TCP. Transplanted tooth germs gave rise to intramembranous bone formation and keratinized cysts. **(F):** Semiquantitative reverse transcription polymerase chain reaction analysis of control or Smad4-siRNA-treated CNCCs (left). X-gal and H&E staining of tooth germs transplanted with Smad4-siRNA-treated CNCCs and HA/TCP. Note that the treatment of CNCCS with Smad4-siRNA resulted in abnormal teeth or cysts. **(G):** H&E staining of T.G. transplanted with BMMSCs, BMP4 beads, and HA/TCP. These T.G. resulted in cyst and bone matrix formation. **(B):** BMP4 beads. Scale bars = 50 $\mu$m. Abbreviations: Alv. Bone, Alveolar bone; B, BMP4 beads; BMMSCs, bone marrow mesenchymal stem cells; BMP4, bone morphogenetic protein 4; CNCCs, cranial neural crest cells; FGF2, fibroblast growth factor 2; FGF4, fibroblast growth factor 4; GF, growth factor containing beads; HA/TCP, hydroxyapatite/tricalcium phosphate; N, noggin beads; PDL, periodontal ligament.